Photophysical Properties of Ruthenium Polypyridyl Photonic SiO_2 Gels

Felix N. Castellano, Todd A. Heimer, Michael T. Tandhasetti, and Gerald J. Meyer*

The Department of Chemistry, Johns Hopkins University, Baltimore, Maryland 21218

Received March 17, 1994. Revised Manuscript Received May 4, 1994®

The photophysical properties of $Ru(bpy)_3(PF_6)_2$ and *cis*-$Ru(bpy)_2(CN)_2$ (where bpy = 2,2′-bipyridine) doped into monolithic SiO_2 aquo and alco gels prepared by sol–gel processing techniques is described. The excited-state properties of the dopants are dramatically altered by the gel matrix. The photoluminescence emission energy and quantum yield of the dopants increase through the sol-to-gel transition. Steady-state fluorescence polarization measurements reveal significant anisotropy. Time-resolved fluorescence decays observed from these photonic materials are complex. Evidence for a bimodal distribution of dopant sites is obtained from modeling the emission decays and from application of the exponential series method. Implications of these results for molecular photonic applications are discussed.

Sol–gel processing represents an attractive technique for the incorporation of thermally unstable compounds within solid state media.[1] Organic dyes,[2] coordination compounds,[3] colloids,[4] and proteins[5] have been successfully "doped" into insulating sol–gel materials. Although these dopants cannot be easily removed from the solid, a significant fraction are exposed to the intrapore region of the solid where they can participate in a diverse variety of chemical reactions. The high transparency of the sol–gel matrix allows this reactivity to be quantitated spectroscopically. Application of sol–gel technology in linear and nonlinear optics, solar energy conversion, sensor technology, and catalysis appears likely.

A particularly intriguing application of sol–gel science for solar energy conversion materials was recently reported by Avnir and co-workers.[6,7] In these studies electron transfer from an excited chromophoric donor, D*, to an electron acceptor, A, was spectroscopically monitored in insulating sol–gel matrices. The products of eq 1 are often

$$D^* + A \xrightarrow{k_{et}} D^+ + A^- \qquad (1)$$

referred to as a charge-separated pair. The importance of these reactions is that they provide a basis for converting light energy into transiently stored, chemical redox energy at the molecular level. Ideally, the charge-separated pair would undergo subsequent processes leading to useful chemical energy products. In solution however, back electron transfer within the solvent cage often limits the lifetime and usefulness of the stored energy.

Avnir and co-workers have largely circumvented this problem by "immobilizing" the donor in a sol–gel matrix and locating a mobile acceptor within the intrapore region of the gel. The mobile acceptor can then shuttle redox energy to a secondary acceptor immobilized in a different location within the gel. The back electron transfer rate is now inhibited by the long distance between the oxidized donor and reduced acceptor. Employing this methodology, charge-separated pairs which live for hours have been produced. In a particularly novel system, back-electron-transfer rates are approximately 7 orders of magnitude slower than those observed in fluid solution.[7] The inorganic sol–gel matrix which contains both an immobilized donor and a mobile redox relay appears to be the key to success.

* Abstract published in *Advance ACS Abstracts,* June 15, 1994.

(1) For recent reviews of sol-gel processing, see: (a) Roy, R. *Science* **1987**, *238*, 1664. (b) Livage, J.; Henry, M.; Sanchez, C. *Prog. Solid State Chem.* **1988**, *18*, 259. (c) Hench, L. L.; West, J. K. *Chem. Rev.* **1990**, *90*, 33. (d) Hench, L. L.; Vasconcelos, W. *Annu. Rev. Mater. Sci.* **1990**, *20*, 269. (e) Dutton, G. F. *Science* **1990**, *249*, 627. (f) Brinker, C. J.; Scherer, G. W. *Sol-Gel Science*; Academic Press: New York, 1991. (g) Martin, J. E.; Adolf, D. *Annu. Rev. Phys. Chem.* **1991**, *42*, 311. (h) Novak, B. M. *Adv. Mater.* **1993**, *5*, 422. (i) Lee, G. R.; Crayston, J. A. *Adv. Mater.* **1993**, *5*, 434.

(2) (a) Reisfeld, R.; Brusilovsky, D.; Eyal, M.; Jorgensen, J. K. *Chimia* **1989**, *43*, 385. (b) Matsui, K.; Matsuzuka, T.; Fujita, H. *J. Phys. Chem.* **1989**, *93*, 4991. (c) Fujii, T.; Mabuchi, T.; Mitsui, I. *Chem. Phys. Lett.* **1990**, *168*, 5. (c) Eyal, M.; Reisfeld, R.; Cherynak, V.; Kaczmarek, L.; Grabowska, A. *Chem. Phys. Lett.* **1991**, *176*, 531. (d) Cherynak, V.; Resifeld, R. *Chem. Phys. Lett.* **1991**, *181*, 39. (e) Devlin, K.; O'Kelly, B.; Tang, Z. R.; McDonagh, C.; McGilip, J. F. *J. Non-Cryst. Sol.* **1991**, *135*, 8. (f) MacCraith, B. D.; Ruddy, V.; Potter, C.; O'Kelly, B.; McGilp, J. F. *Electron. Lett.* **1991**, *27*, 1247. (g) Matsui, K.; Sasaki, K.; Takahashi, N. *Langmuir* **1991**, *7*, 2866. (h) Reisfeld, R.; Jorgensen, J. K. *Struct. Bonding* **1992**, *77*, 207. (i) Liu, H.-Y.; Switalski, S. C.; Coltrain, B. K.; Merkel, P. B. *Appl. Spectrosc.* **1992**, *46*, 1266. (j) Narang, U.; Bright, F. V.; Prasad, P. N. *Appl. Spectrosc.* **1993**, *47*, 229.

(3) (a) Kaufman, V. R.; Avnir, D.; Pines-Rojanski, D.; Huppert, D. *J. Non-Cryst. Sol.* **1988**, *99*, 379. (b) Pouxviel, J. C; Dunn, B.; Zink, J. I. *J. Phys. Chem.* **1989**, *93*, 2134. (c) McKiernan, J.; Pouxviel, J. C.; Novinson, T.; Dunn, B.; Zink, J. I. *J. Phys. Chem.* **1989**, *93*, 2093. (d) Levy, D.; Einhorn, S.; Avnir, D. *J. Non-Cryst. Sol.* **1989**, *113*, 137. (e) Levy, D.; Avnir, D. *J. Phys. Chem.* **1989**, *92*, 4734. (f) Slama-Schwok, A.; Ottolenghi, M.; Avnir, D. *J. Phys. Chem.* **1989**, *93*, 7544. (g) Preston, D.; Pouxviel, J. C.; Novinson, T.; Kaska, W. C.; Dunn, B.; Zink, J. I. *J. Phys. Chem.* **1990**, *94*, 4167. (h) Matsui, K.; Sasaki, K.; Takahashi, N. *Langmuir* **1991**, *7*, 2866. (i) Samuel, J.; Ottolenghi, M.; Avnir, D. *J. Phys. Chem.* **1992**, *96*, 6398.

(4) (a) Schubert, U.; Amberg-Schwab, S.; Breitscheidel, B. *Chem. Mater.* **1989**, *1* 576. (b) Breitscheidel, B.; Zieder, J.; Schubert, U. *Chem. Mater.* **1991**, *3*, 559. (c) Ferrara, C.; Predieri, G.; Tiripicchio, A.; Costa, M. *Chem. Mater.* **1992**, *4*, 243.

(5) (a) Braun, S.; Rappoport, S.; Zusman, R.; Avnir, D.; Ottolenghi, M. *Mater. Lett.* **1990**, *10*, 1. (b) Ellerby, L. M.; Nishida, C. R.; Nishida, F.; Yamanaka, S. A.; Dunn, B.; Valentine, J. S.; Zink, J. I. *Science* **1992**, *255*, 1113. (c) Yamanaka, S. A.; Nishida, F.; Ellerby, L. M.; Nishida, C. R.; Dunn, B.; Valentine, J. S.; Zink, J. I. *Chem. Mater.* **1992**, *4*, 495. (d) Wu, S.; Ellerby, L. M.; Cohan, J. S.; Dunn, B.; El-Sayed, M. A.; Valentine, J. S.; Zink, J. I. *Chem. Mater.* **1993**, *5*, 115.

(6) (a) Slama-Schwok, A.; Ottolenghi, M.; Avnir, D. *J. Phys. Chem.* **1989**, *93*, 7544. (b) Slama-Schwok, A.; Ottolenghi, M.; Avnir, D. *J. Am. Chem. Soc.* **1991**, *113*, 3984. (c) Slama-Schwok, A.; Avnir, D.; Ottolenghi, M. *Photochem. Photobiol.* **1991**, *54*, 525 and references therein.

(7) Slama-Schwok, A.; Ottolenghi, M.; Avnir, D. *Nature* **1992**, *355*, 240.

0897-4756/94/2806-1041$04.50/0

The Avnir approach appears to be very general. Several fundamental questions exist before the application of this advance to practical photocatalytic materials can be realized. For example, how immobilized is an "entrapped" donor? Likewise, how mobile is an electron shuttle? What fraction of the immobilized donors reside in regions where they can participate in electron-transfer reactions with reactants in the intrapore region of the gel? These questions will be better addressed when a detailed knowledge of the local environments of the redox active species is obtained. Furthermore, if one can arrange spatially and isolate the photo- and redoxactive species, the possibility of achieving macroscopic control of directed electron- and energy-transfer processes exists.

In hopes of realizing long-lived charge separation within sol–gel materials, we have turned to the excited-state and redox chemistry of Ru(II) polypyridyl compounds. The solution chemistry of this class of compounds includes electron transfer, energy transfer, and catalysis including the reduction and oxidation of water.[8] Photochemistry is based on metal-to-ligand charge-transfer (MLCT) excited states (eq 2) which have been extremely well characterized in fluid solution.[8] In fact, the parent compound $Ru(bpy)_3^{2+}$ has become a paradigm for inorganic photophysical studies and therefore, represents an excellent starting point for these studies.

$$Ru^{II}(bpy)_3^{2+} \xrightarrow{h\nu} Ru^{III}(bpy^{\bullet-})(bpy)_2^{2+*} \qquad (2)$$

Here we report the steady-state and time-resolved photophysical properties of $Ru(bpy)_3^{2+}$ and *cis*-$Ru(bpy)_2(CN)_2$ in monolithic SiO_2 gels. The Ru(II) compounds were incorporated both before and after gelation in hopes of preparing "immobilized" and "mobile" redox equivalents. The optical properties of the processed materials are in fact sensitive to the preparation conditions. In general, however, the results point toward a complex distribution of environments wherein fully immobilized and mobile environments represent extremes. The distribution can be viewed qualitatively as a partition function. Modeling and application of the exponential series method[9] to the temporal optical properties provides a more insightful quantitative picture of the partition function. The results have implications for the development of chemically integrated photonic materials useful in solar energy conversion.

Experimental Section

Materials Processing. *Materials*: The $Si(OCH_3)_4$ (Aldrich, 98%) and HF (Baker, Reagent Grade) were used as received. Ethanol (Warner-Graham, anhydrous), isopropyl alcohol (Baker, 99.9%), acetone (Baker, 99.6%), diethyl ether (Fisher, anhydrous), formamide (Aldrich, 99+%), dimethylformamide (Baker, 99.5%), dimethyl sulfoxide (Baker, 99.9%), and acetonitrile (Baker, 99.9%) were used as received. Deionized water was obtained from a Barnstead Nanopure System. Methanol (Fisher, spectroscopic grade) was distilled over magnesium turnings under an atmosphere of argon (Roberts Oxygen; 99.99%) after drying over 3-Å molecular sieves. pH measurements were made with an Orion Model 420A pH meter.

$Ru(bpy)_3(PF_6)_2$[10] and *cis*-$Ru(bpy)_2(CN)_2$[11] were prepared and satisfactorily characterized by published methods.

Gel Preparations. Silicon dioxide, SiO_2, sol–gel monoliths were prepared using a variation of a literature preparation.[12] In a 50-mL polystyrene beaker, 2.5 mL of nanopure water were added to a stirred solution of 5.0 mL of tetramethyl orthosilicate and 5.0 mL of freshly distilled methanol in a hood or in a Vacuum Atmospheres drybox. After this stirred for 2 min, 50.0 μL of HF was added with stirring and the solution was pipetted directly into Fisher brand polystyrene cuvettes which were then capped and sealed with parafilm. After 1 day the gels became detached from the polystyrene cuvette walls as optically transparent monoliths. Two days later, they were placed in a 20-mL scintillation vial with either methanol or nanopure water. Volumetric measurements and additions were performed with Ranier brand micropipettemen. Most materials preparation was performed in a N_2-filled Vacuum Atmospheres drybox. In cases where the gels were prepared in the laboratory ambient or exposed to air, they were placed in either a water or methanol bath and bubbled with Ar gas for 24 h prior to spectroscopic analysis.

Ru(II) Incorporated Pregelation. Ruthenium polypyridine compounds were incorporated by dissolving the compound in distilled methanol. This solution was then used as a reactant in place of the neat methanol, as described above in the previous paragraph. After aging 3 days, the gels were transferred into a 20-mL scintillation vial containing either nanopure water or methanol. This solution was changed daily until it did not display room-temperature photoluminescence with black-light excitation.

Ru(II) Incorporated Postgelation. Ru(II) polypyridyl compounds were incorporated into preformed SiO_2 gels which had been aged at least 3 days. The undoped SiO_2 gels were placed in aqueous or methanolic solution containing the compound for 24 h. Incorporation of the complex results in the clear gel turning a yellow color. The gel was then placed in a scintillation vial containing nanopure water or methanol. This solution was changed daily until it was nonemissive with black light excitation.

Optical Characterization. *Absorption Measurements.* The electronic spectrum of all compounds and solids were made on an HP 8451A diode array spectrophotometer, ± 2 nm and ± 0.005 au resolution. Extinction coefficients were measured by preparing a stock solution of $Ru(bpy)_3(PF_6)_2$ in water and *cis*-$Ru(bpy)_2(CN)_2$ in methanol. These solutions were employed in the pre-gelation technique described above. Extinction coefficients were calculated by measuring the absorption spectra immediately after gelation in 1 cm^2 cuvettes. Absorption measurements of sol–gel monoliths employed an alcohol or an undoped gel as the reference.

Steady-State Photoluminescence Measurements. Photoluminescence measurements were made on a home-built fluorimeter. The apparatus consists of a Spectral Energy 150-W Xe lamp coupled to a McPherson *f*/2 monochromator equipped with a holographic grating. Output from the monochromator was coupled via a fiber optic link to a light-tight sample box. Photoluminescence was collected at a right angle with a fiber optic bundle to a second McPherson *f*/2 monochromator. The monochromator was coupled to a thermoelectric cooled housing (Products for Research) equipped with a Hamamastu 943–02 GaAs end-on photomultiplier tube biased at −1900 V with an EMI 3000 R/A power supply. The signal from the photomultiplier tube was amplified and discriminated (Hamamatsu C3866) and sent to a Phillips PM 6680 frequency counter. The frequency counter and monochromators are controlled by a 486 microprocessor via a GPIB interface. A Spex Fluorolog 112, and a Perkin-Elmer LS5 fluorimeter were used to obtain excitation spectra and for some emission measurements. Corrected emission spectra

(8) For recent reviews of MLCT excited states, see: (a) Juris, A.; Barigelletti, F.; Campagna, S.; Balzani, V.; Besler, P.; Von Zelewsky, A. *Coord. Chem. Rev.* **1988**, *84*, 85. (b) Meyer, T. J. *Acc. Chem. Res.* **1989**, *22*, 364. (c) DeArmond, M. K.; Myrick, M. L. *Acc. Chem. Res.* **1989**, *22*, 364. (d) Yersin, H.; Braun, D.; Hensler, G.; Gallhuber, E. In *Vibronic Processes in Inorganic Chemistry*; Flint, C. D., Ed.; Kluwer Academic Publishers: Dordrecht, 1989; p 195. (e) Balzani, V.; Scandola, F. *Supramolecular Photochemistry*; Ellis Harwood: Chichester, UK, 1990. (f) Scandola, F.; Indelli, M. T. *Pure Appl. Chem.* **1988**, *60*, 973.

(9) (a) James, D. R.; Ware, W. R. *Chem. Phys. Lett.* **1986**, *126*, 7. (b) Siemiarczuk, A.; Wagner, B. D. *J. Phys. Chem.* **1990**, *94*, 1661.

(10) Caspar, J. V.; Meyer, T. J. *J. Am. Chem. Soc.* **1983**, *105*, 5583.

(11) Bignozzi, C. A.; Roffia, S.; Chiorboli, C.; Davila, J.; Indelli, M. T.; Scandola, F. *Inorg. Chem.* **1989**, *28*, 4350.

(12) Pope, E. J. A.; MacKenzie, J. D. *J. Non-Cryst. Solids* **1986**, *87*, 185.

were obtained by calibration of the Spex Fluorolog with a NBS standard tungsten–halogen lamp.

Photoluminescence quantum yields were made with $Ru(bpy)_3(PF_6)_2$ as a quantum counter in the optically dilute technique:[13] where ϕ_x, A_x, n_x, and D_x are the quantum yields, absorbance at

$$\phi_x = \phi_r\left(\frac{A_r}{A_x}\right)\left(\frac{n_x}{n_r}\right)^2\left(\frac{D_x}{D_r}\right) \quad (3)$$

the exciting wavelength, refractive index, and integrated photoluminescence intensity for the samples. The corresponding terms with the subscript r are for the $Ru(bpy)_3(PF_6)_2$ reference quantum counter in argon purged water. The photoluminescence quantum yield for $Ru(bpy)_3(PF_6)_2$ under these conditions is $\phi_r = 0.042$.[10] The refractive index of water at this wavelength was extracted from the literature to be 1.3387.[14] The refractive index of the gels was measured as discussed below.[14]

Refractive Index Measurements. The refractive index of freshly prepared gels was measured with 457.9-nm light from an Innova Ar^+ ion laser (Coherent). The collimated laser beam was focused on a hollow prism which contained either a reference solvent or a gel. The refracted laser beam was calibrated with a meter stick approximately 3 m from the sample. Refractive indices at 460 nm used for calibration were extrapolated from literature values.[14] In this manner, refractive indices could be measured to within ±0.0004. Refractive index changes through the sol-to-gel transition were made by pouring the gel reactants into the hollowed prism. Before gelation, n_r was 1.3524 ± 0.0004 and after gelation the refractive index shifted to 1.3537 ± 0.004.

Luminescence Anisotropy. Steady-state fluorescence anisotropy was collected using a SLM 48000 multiple frequency lifetime spectrofluorometer (SLM-Aminco, Urbana, IL). The light excitation source was a Xe lamp (λ_{ex} = 460 ± 4 nm). The focusing lens in the excitation path was removed to reduce sample photobleaching. Fluorescence intensity was proportioned against a rhodamine quantum counter to minimize effects from intensity fluctuations in the lamp. Sample temperatures were maintained at 20 °C using a Neslab TEQ temperature controller and a PCB4 cooler bath. Sample absorbances did not exceed 0.1 at the exciting wavelengths. Measurements were made in the L format with vertically polarized excitation. Anisotropy, $\langle r \rangle$, was calculated as

$$\langle r \rangle = \frac{I_{VV} - GI_{VH}}{I_{VV} + 2GI_{VH}} \quad (4)$$

where I_{VV} and I_{VH} were the measured vertical and horizontal polarized emission intensities, respectively.[15] The G factors were defined by eq 5, which accounts for the different sensitivity of

$$G = I_{HV}/I_{HH} \quad (5)$$

the detection system to vertically and horizontally polarized light. Total emission anisotropy was measured using a Corning 560-nm cut-on filter to eliminate scattered exciting light.

Time-Resolved Photoluminescence Measurements. Time-resolved photoluminescence studies were performed with the apparatus shown schematically in Figure 1. A Laser Photonics LN100/107 nitrogen-pumped dye laser was employed for laser excitation. Coumarin 460 (Exciton) was used as the laser dye and the intensity was monitored with a Molectron J3-09 joulemeter. The exciting light was brought to the sample with a lens system or a fiber optic link. Photoluminescence was collected at a right angle and focused on a $f/3.4$ Applied Photophysics monochromator with two $f/3.4$ lenses. A Hamamatsu R928 photomultiplier tube mounted in an EMI-shielded housing was optically coupled to the monochromator. The base

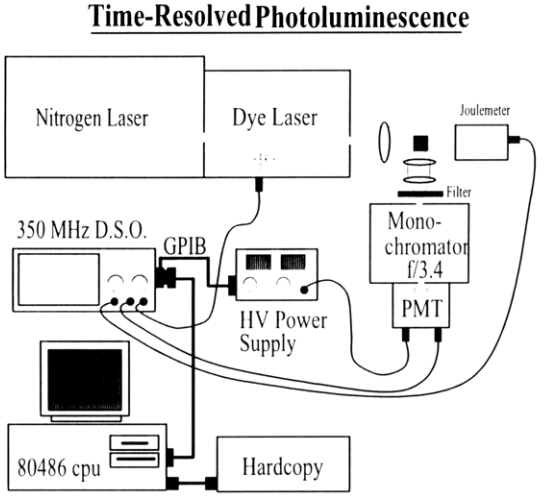

Figure 1. Schematic diagram of the apparatus employed for time resolved photoluminescence measurements. Complete details are given in the Experimental Section.

of the photomultiplier tube was wired for fast response[16] and biased at −800 V with a programmable Stanford Research PS/325 power supply. A reverse-biased PIN (Motorola MRD 500) mounted within the dye laser cavity served as an optical trigger for a LeCroy 9450 digital storage oscilloscope. The oscilloscope was interfaced to a 486-class microprocessor via a GPIB interface. The instrument response function was measured to be 14-ns LUDOX colloidal SiO_2 as a light scatterer.

Results

Gel Preparation. Monolithic SiO_2 gels were prepared by reaction 6.[12] The time required to reach the gel point

$$Si(OCH_3)_4 + 6CH_3OH + 4H_2O \xrightarrow{HF} \rightarrow SiO_2(gel) \quad (6)$$

is highly dependent on the HF concentration.[12,18] Typically, our solutions gel within minutes and display high optical transparency in the visible region. The absorbance for a 1-cm-wide gel is less than 0.1 from 400 to 820 nm and increases rapidly at high energy. The gels are stable and maintain their transparency in ethanol, isopropyl alcohol, acetone, diethyl ether, formamide, dimethylformamide, dimethyl sulfoxide, and acetonitrile. The results presented here are for gels immersed in water and methanol, aquogels and alcogels, respectively. The gel solubility in methanol and water have been reported to be 100 ± 50 ppm under similar conditions.[19] We note that the solubility in water is pH dependent, and the gels can be completely dissolved in 10 M KOH. The pH of the external aqueous solutions of the aquogels is 6.2 ± 0.2.

Ruthenium polypyridyl complexes have been incorporated into the gels by two different techniques referred to as "pregelation" and "postgelation". In the pregelation technique, the Ru(II) compounds were dissolved in the alcohol precursor of reaction 6. The presence of the polypyridyl compounds did not appear to significantly alter the gelation process. In the postgelation technique, undoped gels were prepared, aged for 3 days, and then

(13) Demas, J. N.; Crosby, G. A. *J. Phys. Chem.* **1971**, *75*, 991.
(14) Washburn, E. W., West, C. J., Dorsey, N. E., Ring, M. D., Eds. *International Critical Tables of Numerical Data. Physics, Chemistry, and Technology*, 1st ed.; McGraw Hill: New York, 1930; Vol. 7.
(15) Lakowicz, J. R. *Principles of Fluorescence Spectroscopy*; Plenum Press: New York, 1983.
(16) Harris, J. M.; Lytle, F. E.; McCain, T. C. *Anal. Chem.* **1976**, *48*, 2095.
(17) Gellert, W.; Gottwald, S.; Hellwich, M.; Kastner, H.; Kustner, H. *The VNR Concise Encyclopedia of Mathematics*, 2nd ed.; Van Nostrand Reinhold: New York, 1990.
(18) Winter, R.; Chan, J.-B.; Frattini, R.; Jonas, J. *J. Non-Cryst. Solids* **1988**, *105*, 214.
(19) Iler, R. K. *The Chemistry of Silica*; Wiley: New York, 1979.

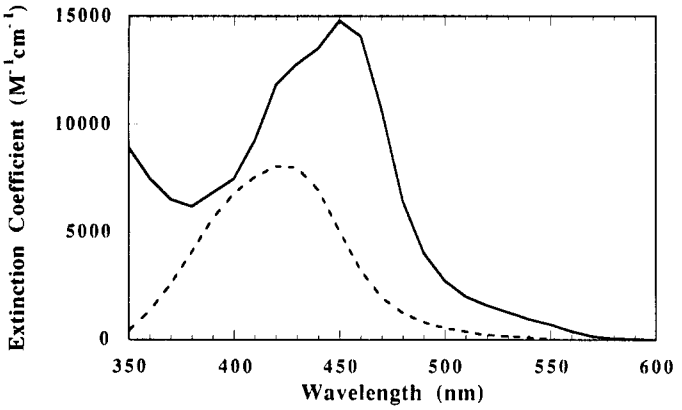

Figure 2. Visible absorption spectra of $Ru(bpy)_3(PF_6)_2$ (solid line) and $Ru(bpy)_2(CN)_2$ (dashed line) SiO_2 aquogels.

placed in aqueous or methanolic solutions containing the Ru(II) polypyridyl dopants. In both techniques, after Ru(II) incorporation, the gels were placed in 20 mL of neat methanol or water which was changed daily until it was no longer luminescent. Generally, the external solution was nonemissive after 3 days of solvent exchange. $Ru(bpy)_2(CN)_2$ can be completely removed from the gel matrix by methanol as evidenced by the resultant transparent nonemissive alcogel. The loss of $Ru(bpy)_3^{2+}$ from the gel matrix is minimal in both methanol and water.

Steady-State Optical Properties. The absorbance spectra of $Ru(bpy)_3(PF_6)_2$ and *cis*-$Ru(bpy)_2(CN)_2$ incorporated in SiO_2 aquogels is shown in Figure 2. The absorption spectra remain unchanged over periods of months independent of whether the Ru(II) compounds were incorporated before or after gelation. The $\pi-\pi^*$ transitions of the bipyridine ligands are obscured by gel absorption, but the broad MLCT transitions are clearly visible. The MLCT absorption maximum for $Ru(bpy)_3(PF_6)_2$ is 452 ± 2 nm in alcogels, aquogels, and solutions of methanol or water. The MLCT absorption maximum of $Ru(bpy)_2(CN)_2$ is 426 ± 2 nm in water and aquogels. $Ru(bpy)_2(CN)_2$ is highly solvatochromic,[8f] and the absorption maximum shifts dramatically in methanol. However, as is discussed above, the compound is completely extracted from the gel in methanol making comparisons difficult.

Excitation into the broad MLCT absorption results in room-temperature photoluminescence. Figure 3 displays the corrected normalized emission and excitation spectra of the doped aquogels from Figure 2. Gels which did not contain Ru(II) are nonemissive under these conditions. Polarization studies reveal significant luminescence anisotropy, $\langle r \rangle$. Measured anisotropy values are independent of observation wavelength from 550 to 700 nm within experimental error. Therefore, we generally monitored the total integrated anisotropy over these energies. Complete photophysical characteristics of the materials are summarized in Table 1.

The optical properties of $Ru(bpy)_3(PF_6)_2$ and *cis*-$Ru(bpy)_2(CN)_2$ through the sol-to-gel transition were explored by adding catalyst to the Ru(II)-containing reactants during continuous optical measurements. With this methodology, no significant changes were observed in the Ru(II) absorption spectrum. The photoluminescence quantum yield increases and the corrected maximum shifts to higher energy during and after the gel point (Figure 4). The full width at half-maximum remains constant through this transition at 3060 cm^{-1} for $Ru(bpy)_3^{2+}$ and 3400 cm^{-1}

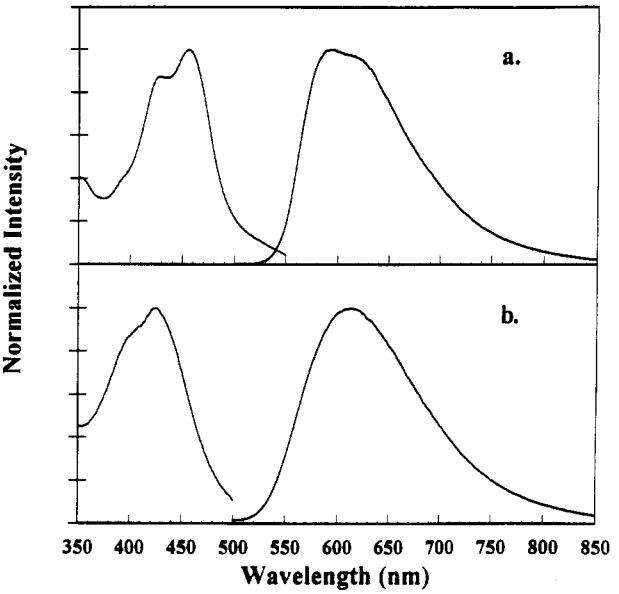

Figure 3. Corrected excitation and emission spectra of (a) $Ru(bpy)_3(PF_6)_2$ and (b) $Ru(bpy)_2(CN)_2$ aquogels. The Ru(II) compounds were incorporated into the gels prior to gelation.

for $Ru(bpy)_2(CN)_2$ (Figure 4). The refractive index increases by $\sim 10^{-3}$ through this transition, which could only account for <2% increase in the measured quantum yield. No dramatic optical changes occur right at the gel point. The most rapid emission energy shifts occur immediately after the addition of catalyst. Qualitatively, the more catalyst added the more rapidly the optical properties of the gel change.

Temporal Optical Properties. The photoluminescence decays from $Ru(bpy)_3^{2+}$ doped into SiO_2 gels before and after gelation are nonexponential. The decays are insensitive to the observation wavelength, excitation irradiance from 0.9 to 90 μJ/pulse, and the chromophore concentration within the limits of solubility. Luminescence decays from $Ru(bpy)_2(CN)_2$ doped aquogels are also nonexponential. The emission spectral distribution is unchanged after excitation with a laser pulse. Figure 5 displays the uncorrected photoluminescence spectra between 20 ns and 2 μs for the $Ru(bpy)_3^{2+}$ aquogel from Figure 2.

The photoluminescence decays can be adequately described by a sum of two exponential decays or by the Kohlrausch–Williams–Watts, KWW, function.[20] Figure 6 displays the luminescence decay of a $Ru(bpy)_3^{2+}$ aquogel fit to these models. The KWW function is given in eq 7,

$$I(t) = \alpha \exp[-(t/\tau)^{\beta}] \tag{7}$$

where the parameter β ($0 < \beta < 1$) is related to the width of an underlying Levy distribution of relaxation rates, and τ is the lifetime at the maximum amplitude of the distribution. The biexponential model is given by eq 8,

$$I(t) = \sum_{i=1}^{2} \alpha_i \exp[-(t/\tau_i)] \tag{8}$$

and the average lifetime are calculated by taking the first moment of the functions. Equation 9 is the first moment

(20) (a) Kohlrausch, R. *Ann.* **1847**, *5*, 430. (b) Williams, G.; Watts, D. C. *Trans. Faraday Soc.* **1971**, *66*, 80.

Table 1. Photoluminescent Properties of SiO_2 Photonic Gels

					biexponential model			KWW model		
assembly[a]	λ_{max} PL[b] (nm)	Φ[c]	$\langle r \rangle$[d]	τ (ns)	τ_1 (α_1) (μs)	τ_2 (α_2) (μs)	$\langle \tau' \rangle$ (μs)	β	τ (μs)	$\langle \tau \rangle_{KWW}$ (μs)
$Ru(bpy)_3/H_2O$	627	0.042	0.0009	578						
$Ru(bpy)_3$/MeOH	609	0.045		851						
$Ru(bpy)_2(CN)_2/H_2O$	634	0.0085	0.0014	259						
$Ru(bpy)_3/SiO_2/H_2O$/pre	590	0.062	0.1059		1.68 (0.069)	0.581 (0.31)	1.53	0.843	1.18	1.30
$Ru(bpy)_3/SiO_2/H_2O$/post	604		0.0745		1.06 (0.77)	0.353 (0.24)	0.983	0.872	0.813	0.871
$Ru(bpy)_3/SiO_2$/MeOH/pre	582	0.094	0.1149		2.25 (0.60)	0.503 (0.40)	2.02	0.706	1.17	1.47
$Ru(bpy)_3/SiO_2$/MeOH/post	604		0.0778		1.31 (0.50)	0.617 (0.53)	1.08	0.857	0.824	0.892
$Ru(bpy)_2(CN)_2/SiO_2/H_2O$/pre	614	0.027	0.1799		0.488 (0.59)	0.158 (0.55)	0.410	0.727	0.236	0.288
$Ru(bpy)_2(CN)_2/SiO_2/H_2O$/post	616		0.1778		0.446 (0.54)	0.168 (0.60)	0.365	0.750	0.218	0.260

[a] Assemblies denoted pre and post are for those prepared with the pregelation and postgelation techniques, respectively. [b] Corrected photoluminescence spectra with 460-nm excitation, ±4 nm. [c] Photoluminescence quantum yield calculated with eq 3. [d] Steady-state fluorescence anisotropy measured at 20 °C.

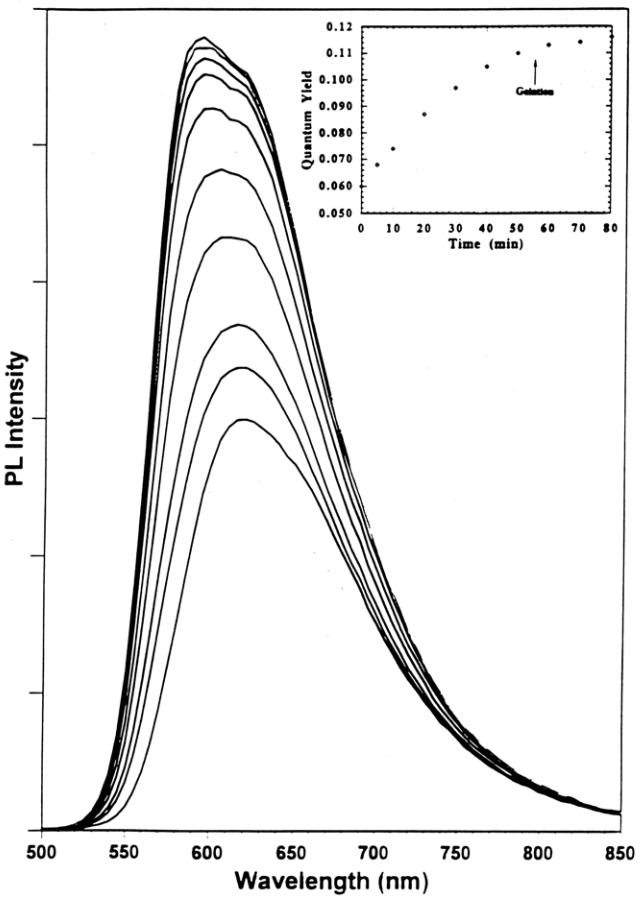

Figure 4. Corrected photoluminescence spectra of $Ru(bpy)_3(PF_6)_2$ 0, 5, 10, 20, 30, 40, 50, 60, 70, and 80 min after the addition of HF catalyst. The bottom spectrum was obtained at time equals 0 and increases monotonically with time. The inset shows the photoluminescence quantum yield as a function of time. The sample gelled after 50 min and was excited with 460-nm light. Other details are given in the Experimental Section.

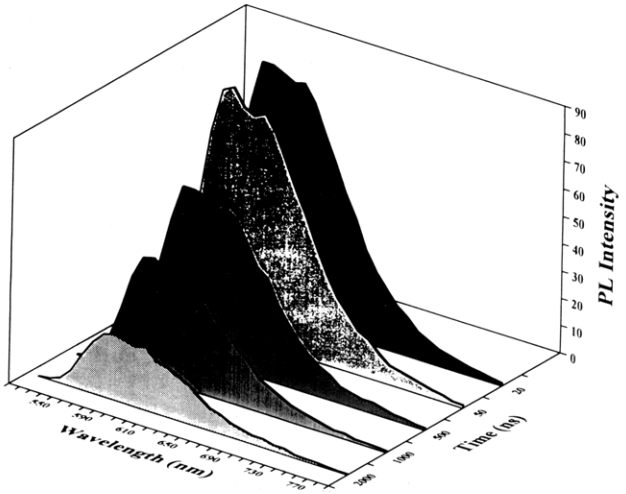

Figure 5. Uncorrected photoluminescence spectra of a $Ru(bpy)_3(PF_6)_2$ aquogel 20, 50, 500, 1000, and 2000 ns after excitation with a subnanosecond pulse of 460-nm light.

of the biexponential model and eq 10 is the first moment of the KWW model.[21] Γ represents the gamma function.

$$\langle \tau \rangle_{bi} = \sum_{i=1}^{2} \alpha_i \tau_i^2 / \sum_{i=1}^{2} \alpha_i \tau_i \qquad (9)$$

$$\langle \tau \rangle_{KWW} = (\tau/\beta)\Gamma(1/\beta) \qquad (10)$$

Average lifetimes, based on the first moments of the KWW and biexponential models for $Ru(bpy)_3^{2+}$ and $Ru(bpy)_2(CN)_2$ incorporated pre- and postgelation are summarized in Table 1. The photoluminescence decays could not be modeled by a single normal (Gaussian) or Lorentzian distribution of lifetimes.[17] Reconstructed synthetic decays, with appropriate signal to noise, based on these distributions could be satisfactorily fit to both the KWW and biexponential models. However, fits to the biexponential model could not reproduce the experimentally observed difference in rates and fits to the KWW model could not produce β values <0.9, with these lifetimes. The full width at half-maximum of these distributions is often limited since significant amplitude exists at time equal to zero. The distributions were generally truncated when they reached 10^{-4} of their peak amplitude. While a single symmetric distribution could not model the data, a variety of single asymmetric distributions and sums of Gaussians, Lorentzians, or individual rates will model the experimental data.

The exponential series method, ESM, was applied to the complex photoluminescence decays observed in these photonic materials. This method has been previously discussed, analytically tested, and implemented by Ware and co-workers.[9] A few notes on our implementation techniques are useful. Initially, the decay is modeled by a uniformly weighted probe function of 21 lifetimes of variable density evenly spaced in time. An estimation of the minimum rate limit was crudely assessed by the time scale of the decay. The fast rate limit was more difficult to assess. We have found, for the systems at hand, that rates faster than 10^8 s^{-1} do not improve the quality of the fit. The Euclidean norm of the objective function, the

(21) Linsey, C. P.; Patterson, G. D. *J. Chem. Phys.* **1980**, *73*, 3348.

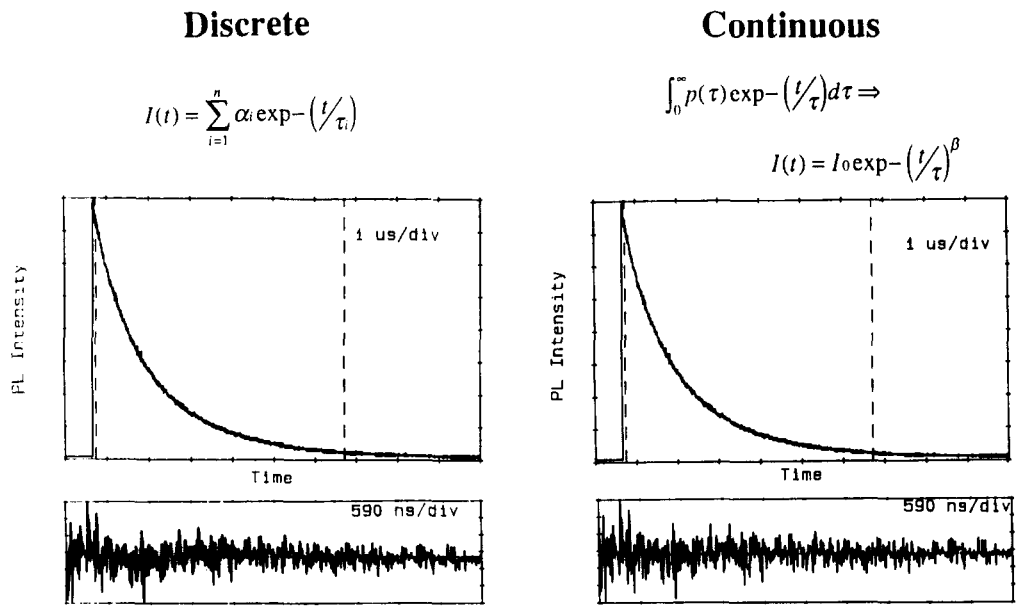

Figure 6. Time-resolved photoluminescence spectra of a a $Ru(bpy)_3(PF_6)_2$ aquogel. The left-hand panel represents a fit to a discrete model with $n = 2$ rates. The right-hand panel represents a fit to a continuous model based on the Kohlrausch–Williams–Watts model. Residuals are shown to judge the quality of the fit.

data with respect to the probe function, is then minimized by a Nelder–Mead modified simplex procedure. The results of such a study are shown in Figure 7 for $Ru(bpy)_3^{2+}$ incorporated in an SiO_2 gel by the pregelation technique. Note that all rates faster than $\sim 2.5 \times 10^6$ s^{-1} and slower than $\sim 1.0 \times 10^5$ s^{-1} are eliminated by the ESM. The same analysis on a large number of photonic materials consistently revealed a bimodal distribution of rates. We found that the number of rates recovered and their relative amplitudes is dependent on the density of the probe function, the initial and final limits, and the convergence criteria. At this probe density the recovered rates were not highly dependent on the signal-to-noise ratio.

Discussion

The results demonstrate clearly that $Ru(bpy)_3^{2+}$ and *cis*-$Ru(bpy)_2(CN)_2$ can be incorporated into monolithic SiO_2 gels to produce photonic materials with interesting optical properties. An initial goal was to prepare photonic materials in which the dopants were either mobile or fully entrapped within the sol–gel matrix. This goal was not realized. Instead, the Ru(II) dopants seem to partition themselves in a distribution of environments. The microenvironments perturb the MLCT excited states of the dopants in a manner which can be largely rationalized based on previous measurements in fluid solution and low-temperature glasses. The inherent heterogeneity of these materials leads to complex kinetic behavior which can be better understood through modeling. These observations are important as they further demonstrate the potential for probing sol–gel environments on a molecular level.

Steady-State Optical Properties. The absorption spectra of the Ru(II) compounds are largely preserved before and after gelation, while the photoluminescence properties are dramatically altered by the gel matrix. This perturbation manifests itself in the blue-shifted emission maximum, higher emission quantum yields, and the appearance of nonexponential emission decays with long average lifetimes. Quantitatively, the photoluminescence properties for materials with the dopants incorporated

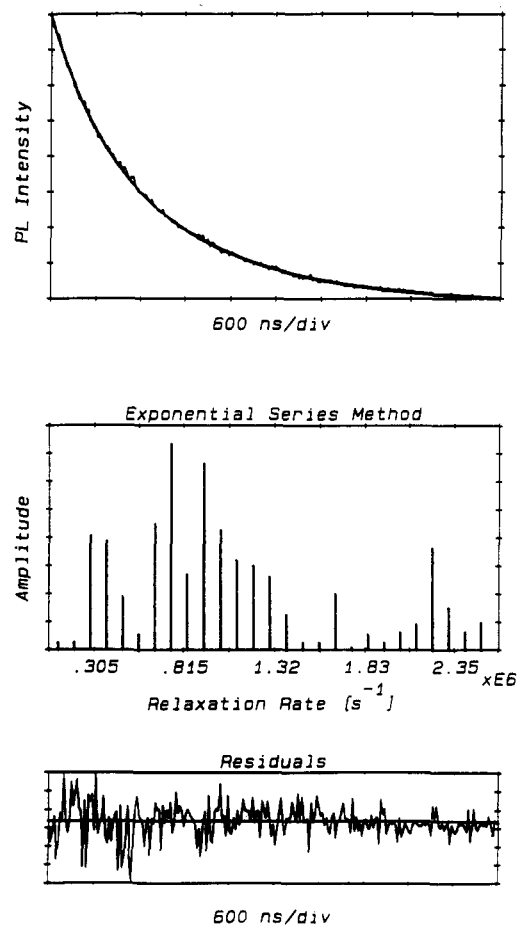

Figure 7. Top: time-resolved photoluminescence decay from a $Ru(bpy)_3(PF_6)_2$ aquogel. Superimposed on these data is a synthetic decay reconstructed from the distribution of rates recovered from the ESM. These rates are shown in the central panel. Residuals to the fit are also shown. Complete details are given in the text.

pregelation are more dramatically changed from their solution values than those incorporated postgelation. This remains true even if the gels are aged for months before

dopant incorporation. Table 1 summarizes the photoluminescence properties of aquo- and alcogels in nonluminescent water and alcohol, respectively.

The photoluminescence maximum shifts toward higher energy through and after the sol-to-gel transition. This phenomena has been observed previously with charge-transfer compounds doped into sol–gel processed photonic materials.[3b,h] The emission maximum from dopants incorporated postgelation are also blue shifted, but to a lesser extent. Luminescence energy shifts with changes in environment have been previously observed in MLCT excited states, and the effect was originally termed "rigidochromism".[22] Detailed studies since that time have shown this to be a general phenomenon due to dipole reorientation time scales.[23] The basis for this is as follows: Dipoles in the vicinity of a chromophore must reorientate in response to the immediate change in electronic structure induced by light excitation. In fluid solution this reorientation is fast and the chromophore emits light from a relaxed excited state. In the solid state or in viscous media, dipole reorientation times often become competitive with the excited-state decay and a time-dependent red shift in the emission spectra results. Our inability to observe such a shift on a nanosecond time scale indicates that dipole reorientation is still fast in the gel matrix, $>7 \times 10^7$ s^{-1}. In contrast, steady-state fluorescence polarization measurements reveal significant anisotropy for the Ru(II) compounds doped into the gels. The anisotropy values are highest for $Ru(bpy)_2(CN)_2$ incorporated pregelation but do not reach the limiting value of 0.40 expected when the transition moments are collinear.[15] The results here indicate that Ru(II) mobility is restricted while dipole reorientation remains fast, even when the chromophores are incorporated postgelation.

The processed photonic materials have a high quantum yield for emission. Measurements through the sol-to-gel transition demonstrate that the quantum yield increases markedly. The increase can not be explained by changes in refractive index, temperature, or oxygen content. In qualitative agreement with the energy gap law,[24] the photoluminescence maximum blue shifts with the increase in quantum yield. This law predicts an exponential decrease in the nonradiative rate constant, k_{nr}, with increasing energy gap. The energy gap for MLCT excited states is approximately the energetic difference between the bipyridine reduction potential and the $Ru^{III/II}$ couple. Crudely approximating the energy gap as the photoluminescence onset,[8] for $Ru(bpy)_3^{2+}$ the energy gap increases from 2.23 eV before gelation to 2.29 eV after. With these data it is difficult to predict whether the ground state, excited states, or both are stabilized. However, recent electrochemical measurements of $Ru(bpy)_3^{2+}$ doped sol–gel processed SiO_2 films demonstrate that the ground-state potential is unchanged from its solution value.[25] If this observation can be extended to the monolithic gels studied here, this and the unperturbed absorption spectra would indicate that the excited states of $Ru(bpy)_3^{2+}$ and $Ru(bpy)_2(CN)_2$ are destabilized with respect to their solution analogs. While the observed energy shift is too small to accurately test the energy gap law, the results are also consistent with a decrease in the nonradiative rate constants of Ru(II) polypyridyl compounds in the gel matrix.

Temporal Photoluminescence Properties. The excited-state temporal properties of Ru(II) polypyridyl-doped gels are complex. Specifically, nonexponential emission decays are routinely observed. Only in the very early stages of gel formation can the temporal optical properties be modeled by a single exponential decay. A fundamental question is, are the nonexponential decays a result of several discrete rates or is there an underlying distribution of rates? Initially we hoped to answer this question by fitting our data to a sum of discrete rates and to the Kohlrausch or Williams–Watts (KWW) model which can be derived from a continuous distribution of rates.[26] Statistically however, we cannot distinguish which model more accurately reproduces the observed data summarized in Table 1. In addition, reconstructed synthetic decay signals, based on a single normal or Lorentzian distribution, with appropriate signal-to-noise, are unable to model our experimental data.[27] While symmetric distributions cannot approximate the observed data, an asymmetric (skewed) distribution or a sum of two or more distributions can. By this modeling we concluded that there exists either a single skewed distribution of decay rates or a sum of several unknown distributions.

To gain more insight into the fundamental nature of the complex kinetic decays, we implemented the exponential series method, ESM, developed by Ware and co-workers.[9] This method directly recovers distributions of rates from complex fluorescence decays. For Ru(II)-doped photonic materials, ESM analysis consistently recovers a bimodal distribution of rates and not a single skewed distribution. However, in our hands ESM fails to identify the underlying analytical nature of the two distributions. This inadequacy is undoubtedly due to the fact that there are a large number of distributions which can adequately describe our data. Nevertheless, ESM consistently recovers a bimodal distribution of rates which is consistent with our modeling studies. The peak amplitude in the faster rate corresponds approximately to the rate recovered prior to addition of catalyst, and the slower distribution of rates may correspond to Ru(II) compounds well entrapped within the gel. This picture is also consistent with a distribution of low and high microviscosity domains, as suggested by Bright and co-workers for rhodamine 6G in SiO_2 gels.[28] This conclusion is important as it indicates that average lifetimes, calculated as first moments, correspond to rates with little or no amplitude and are therefore of limited value.

It still remains uncertain what holds the Ru(II) dopants within the gel matrix. At this pH the silica surface is negatively charged.[19] The incorporation of $Ru(bpy)_3^{2+}$ could therefore, be entirely electrostatic in nature. In fact, if an aged gel is placed in a dilute aqueous $Ru(bpy)_3^{2+}$ solution, all the compound is incorporated in the gel, much like "thirsty" Vycor glass.[29] The neutral *cis*-$Ru(bpy)_2(CN)_2$ could bind to surface H^+ groups through the ambidentate CN^- ligand, however, this is expected only

(22) Wrighton, M.; Morse, D. L. *J. Am. Chem. Soc.* **1974**, *96*, 998.
(23) Marcus, R. A. *J. Phys. Chem.* **1990**, *94*, 4963 and references therein.
(24) Jortner, J. *J. Chem. Phys.* **1970**, *52*, 6272.
(25) Dvorak, O.; DeArmond, M. K. *J. Phys. Chem.* **1993**, *97*, 2646.
(26) (a) Scher, H.; Shlesinger, M. F.; Bendler, J. T. *Phys. Today* **1991**, *588*, 26 and references therein. (b) Palmer, R. K.; Stein, D.; Abrahams, E. S.; Anderson, P. W. *Phys. Rev. Lett.* **1984**, *53*, 958.
(27) Albery, W. J.; Bartlett, P. N.; Wilde, C. P.; Darwent, J. R. *J. Am. Chem. Soc.* **1985**, *107*, 1854.
(28) Narang, U.; Wang, R.; Prasad, P. N.; Bright, F. V. *J. Phys. Chem.* **1994**, *98*, 17.
(29) Gaffney, H. *Coord. Chem. Rev.* **1990**, *104*, 113 and references therein.

at pH < 1.[30] Furthermore, the stability of $Ru(bpy)_3^{2+}$-doped within SiO_2 at high ionic strength and at pH = 0.5, below the isoelectronic point, indicates that electrostatics alone cannot explain dopant binding.

An alternative way of viewing the distribution of dopant molecules within the gel matrix is as a partition coefficient, K. The use of partition coefficients ignores the specific chemical interactions responsible for binding but has been useful for obtaining a better understanding of the distribution of molecules at interfaces.[31] Consider the simple case where a dopant molecule D resides in the external pore solvent, D_p, or is embedded in the polymeric SiO_2, D_s:

$$D_s \overset{K}{\leftrightarrow} D_p \tag{11}$$

The photonic gels seem to follow this simple picture, although clearly a distribution of pores and surface sites exist. For *cis*-$Ru(bpy)_2(CN)_2$ alcogels the partition coefficient favors the pores and this compound can be completely removed from the gel, while for $Ru(bpy)_3^{2+}$ aquogels the SiO_2 matrix is favored. Our results suggest that dopants incorporated after gelation establish this same partioning with some SiO_2 surface sites no longer accessible. For photonic applications which require a mobile redox shuttle, species with a high affinity for the external solvent are required. Likewise, for applications which require a fully immobilized dopant, species with a high affinity for SiO_2 are required. In general, this could be accomplished by incorporation of a dopant which is insoluble in the external solvent or through covalent attachment.

(30) (a) Peterson, S. H.; Demas, J. N. *J. Am. Chem. Soc.* **1976**, *98*, 7880. (b) Demas, J. N.; Addington, J. W.; Peterson, S. H.; Harris, E. W. *J. Phys. Chem.* **1977**, *81*, 1039. (c) Peterson, S. H.; Demas, J. N. *J. Am. Chem. Soc.* **1979**, *101*, 6571. (d) Bignozzi, C. A.; Scandola, F. *Inorg. Chem.* **1984**, *23*, 1540. (e) Davila, J.; Bignozzi, A. A.; Scandola, F. *J. Phys. Chem.* **1989**, *93*, 1373.

(31) MacRitchie, F. *Chemistry at Interfaces*; Academic Press: San Diego, 1990.

Conclusions

The successful preparation and photophysical characterization of $Ru(bpy)_3(PF_6)_2$ and *cis*-$Ru(bpy)_2(CN)_2$ doped into monolithic SiO_2 has been described. The excited-state properties of the dopants are dramatically altered by the gel matrix. The corrected photoluminescence energy maximum and quantum yield increase through the sol-to-gel transition. The higher energy emission is thought due to stabilization of the dopant excited state and the increased quantum yield is a consequence of the energy gap law. The rotational dynamics of the compounds are hindered in the gel matrix. Strong evidence for a bimodal distribution of dopant sites is obtained from modeling the emission decays and from application of the exponential series method. The partioning of the dopants between these environments is dependent on the nature of the dopant, the solvent, and the sol–gel processing conditions.

Acknowledgment. We would like to thank the Hamamatsu Corporation for the generous donation of the photon-counting apparatus.